

A length scale for the superconducting Nernst signal above T_c in $\text{Nb}_{0.15}\text{Si}_{0.85}$

A. Pourret¹, H. Aubin¹, J. Lesueur¹, C. A. Marrache-Kikuchi², L. Bergé², L. Dumoulin², K. Behnia¹

(1) *Laboratoire de Physique Quantique(CNRS), ESPCI, 10 Rue de Vauquelin, 75231 Paris, France*

(2) *CSNSM, IN2P3-CNRS,Bâtiment 108, 91405 Orsay, France*

(Dated: January 11, 2007)

We present a study of the Nernst effect in amorphous superconducting thin films of $\text{Nb}_{0.15}\text{Si}_{0.85}$. The field dependence of the Nernst coefficient above T_c displays two distinct regimes separated by a field scale set by the Ginzburg-Landau correlation length. A single function $F(\xi)$, with the correlation length as its unique argument set either by the zero-field correlation length (in the low magnetic field limit) or by the magnetic length (in the opposite limit), describes the Nernst coefficient. We conclude that the Nernst signal observed on a wide temperature ($30 \times T_c$) and field ($4 \times B_{c2}$) range is exclusively generated by short-lived Cooper pairs.

PACS numbers: 74.70.Tx, 72.15.Jf, 71.27.+a

The observation of a finite Nernst signal in the normal state of high- T_c cuprates[1] has revived interest in the study of superconducting fluctuations. In low-temperature conventional superconductors, short-lived Cooper pairs above T_c have been mostly examined through the phenomena of paraconductivity[2] and fluctuation diamagnetism[3]. Due to a sizeable contribution coming from free electrons to conductivity and magnetic susceptibility, the sensitivity of these probes to superconducting fluctuations is limited to a narrow region close to the superconducting transition[4].

Because of a low superfluid density, the superconducting state in underdoped cuprates is particularly vulnerable to phase fluctuations[5]. Therefore, long-lived Cooper pairs without phase coherence and vortex-like excitations associated with them were considered as the main source of the anomalous Nernst effect observed in an extended temperature window above T_c in underdoped cuprates[1].

In a recent experiment on amorphous thin films of the conventional superconductor $\text{Nb}_{0.15}\text{Si}_{0.85}$ [6], we found that a Nernst signal generated by short-lived Cooper pairs could be detected up to very high temperatures ($30 \times T_c$) and high magnetic field ($4 \times B_{c2}$) in the normal state. In these amorphous films, the contribution of free electrons to the Nernst signal is negligible. Indeed, the Nernst coefficient of a metal scales with electron mobility[7]. The extremely short mean free path of electrons in amorphous $\text{Nb}_{0.15}\text{Si}_{0.85}$ damps the normal-state Nernst effect and allows a direct comparison of the data with theory. In the zero-field limit and close to T_c , the magnitude of the Nernst coefficient was found to be in quantitative agreement with a theoretical prediction[8] by Ussishkin, Sondhi and Huse, (USH) invoking the superconducting correlation length as its single parameter. At high temperature and finite magnetic field, the data was found to deviate from the theoretical expression.

In this Letter, we extend our measurements and analysis of the Nernst signal to high magnetic field and temperatures well above T_c . The Nernst coefficient, ν , is reduced as one increases either the temperature or the magnetic field. We will show here that both

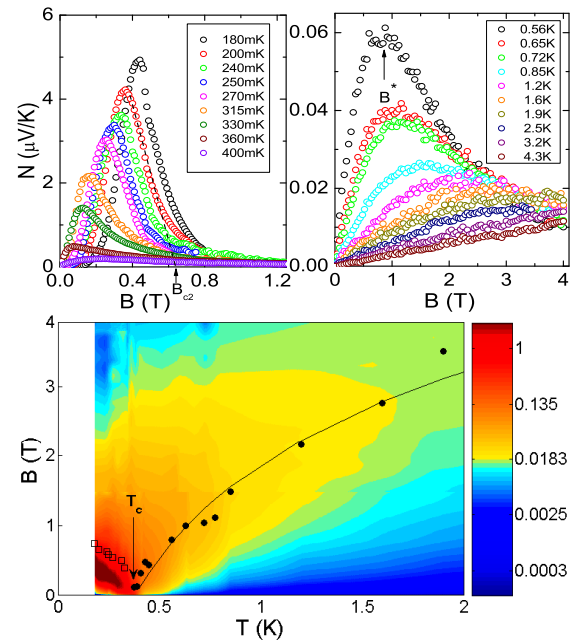


FIG. 1: The Nernst signal (N) as a function of magnetic field for temperatures ranging from 0.180 K to 0.360 K (Upper left panel) and from 0.56 to 4.3 K (Upper right panel) measured on sample 2 ($T_c=380$ mK). Above (below) T_c the position of the maximum in the field dependence of the Nernst signal increases (decreases) with decreasing temperature. Lower panel : Logarithmic color map of the Nernst signal in the (B, T) plane. Superimposed on the plot are the values of the critical field (open squares), below T_c , and B^* (full circles), above T_c . Note the symmetric evolution of these two with respect to T_c . The continuous line is the field scale set by the Ginzburg-Landau correlation length, $B^* = \frac{\phi_0}{2\pi\xi_d}$.

these variations reflect a unique dependence on a single length scale. A striking visualization of this emerges when one substitutes temperature and magnetic field by their associated length scales: the zero-field superconducting correlation length $\xi_d(T)$ and the magnetic length $l_B(B) = (\hbar/2eB)^{1/2}$. The symmetric contour lines of ν in the (l_B, ξ_d) plane shows that its dependence on both

field and temperature can be described by a single function with the superconducting correlation length ξ as its unique argument. In the low-field limit, the correlation length is set by ξ_d and in the high-field limit by l_B . In the intermediate regime, when $\xi_d \simeq l_B$, the correlation length is a simple combination of these two lengths. This observation is additional proof that the Nernst signal observed up to high temperature ($30 \times T_c$) and high magnetic field ($4 \times B_{c2}$) in this system is exclusively generated by superconducting fluctuations – i.e. short-lived Cooper pairs. Hence the functional dependence of the Nernst coefficient on the correlation length is empirically determined in a wide range extending from the long correlation length regime, where the data follows the prediction of USH theory, to the short correlation length regime, where the Ginzburg-Landau approximation fails and no theoretical expression is yet available.

Amorphous thin films of $\text{Nb}_x\text{Si}_{1-x}$ were prepared in ultrahigh vacuum by electron beam co-evaporation of Nb and Si, with special care over the control and homogeneity of the concentrations. The competition between superconducting, metallic and insulating ground states is controlled by the Nb concentration, the thickness of the films, or the magnetic field[9, 10, 11]. Two samples of identical stoichiometry – $\text{Nb}_{0.15}\text{Si}_{0.85}$ – but with different thicknesses and T_c are used in this study. Sample 1 (2) was 12.5 (35) nm thick and its midpoint T_c was 0.165 (0.380) K. The physical properties of these two samples as well as the experimental set-up were detailed in our previous communication, which also presented part of the data discussed here[6].

Figure 1 shows the Nernst signal, $N = \frac{E_y}{(-\nabla_x T)}$ as a function of magnetic field and temperature, for sample 2. Below T_c , the magnetic field dependence shows the characteristic features of vortex-induced Nernst effect, well known from previous studies on conventional superconductors[12] and high- T_c cuprates[1]. For each temperature, the Nernst signal increases steeply when the vortices become mobile following the melting of the vortex solid state. It reaches a maximum and decreases at higher fields when the excess entropy of the vortex core is reduced. As the temperature decreases the position of this maximum shifts towards higher magnetic fields. This is not surprising, since in the superconducting state, all field scales associated with superconductivity are expected to increase with decreasing temperature. In particular, this is the case of the upper critical field, B_{c2} , which can be roughly estimated by a linear extrapolation of the Nernst signal to zero as it has been done in cuprates[1].

Above T_c , the temperature dependence of the characteristic field scale is reversed. In this regime, at low magnetic field, the Nernst signal $N = R_{\text{square}} \times \alpha_{xy}$ increases linearly with field, as expected from the USH theory where α_{xy} follows the simple expression[8] :

$$\alpha_{xy} = \frac{1}{3\pi} \frac{k_B e}{\hbar} \frac{\xi^2}{l_B^2} \quad (1)$$

[Note that here we use the definition of $l_B(B) = (\hbar/2eB)^{1/2}$, which differs by a factor of $\sqrt{2}$ from what was used in ref.[8] and [6]. This, for obvious reasons to appear below.] Upon increasing the magnetic field, the Nernst signal deviates from this linear field dependence, reaches a maximum at a field scale B^* and decreases afterwards to a weakly temperature-dependent magnitude. In contrast to the superconducting state ($T < T_c$), the position of the maximum shifts to higher fields with increasing temperature. The contour plot in the (T,B) plane (lower panel) shows that these two field scales, B_{c2} and B^* , evolve symmetrically with respect to the critical temperature. One major observation here is that the magnitude and the temperature dependence of B^* follows the field scale set by the Ginzburg-Landau correlation length $\xi_d = \frac{\xi_{0d}}{\sqrt{\epsilon}}$ through the relation $B^* = \frac{\phi_0}{2\pi\xi_d^2}$ where ϕ_0 is the flux quantum and $\epsilon = \ln \frac{T}{T_c}$ the reduced temperature. [This field scale was dubbed “the ghost critical field” by Kapitulnik and co-workers[13].] The value for the correlation length at zero-temperature ξ_{0d} is determined from the BCS formula in the dirty limit $\xi_{0d} = 0.36 \sqrt{\frac{3}{2} \frac{\hbar v_F \ell}{k_B T_c}}$, where $v_F \ell = 4.35 \times 10^{-5} \text{ m}^2 \text{s}^{-1}$ is estimated using the known values of electrical conductivity and specific heat[6]. Thus, the decrease of the Nernst

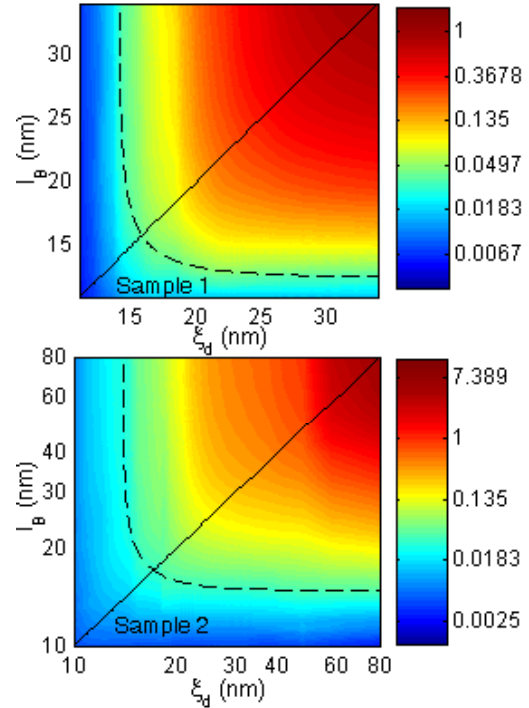


FIG. 2: Logarithmic color map of the Nernst coefficient as a function of the magnetic length l_B and the zero-field correlation length ξ_d , for sample 1 (upper panel) and sample 2 (lower panel). Note the symmetry of the Nernst coefficient with respect to the diagonal continuous line ($l_B = \xi$). Dots lines represents contours for $\xi = 15 \text{ nm}$ with $\xi = (1/\xi_d^4 + 1/(c \times l_B)^4)^{-1/4}$. $c = 1.12$ for sample 1 and $c = 0.93$ for sample 2.

signal at the field scale B^* is the consequence of the reduction of the correlation length when the cyclotron diameter l_B becomes shorter than the zero-field correlation length ξ_d , at a given temperature. This phenomena is well known from studies of fluctuations diamagnetism in low temperature superconductors[3] and cuprates[14]. While in the low field limit, the magnetic susceptibility should be independent of the magnetic field – i.e. in the Schmidt limit[15] –, the magnetic susceptibility is experimentally observed to decrease with the magnetic field, following the Prange's formula[16]; which is an exact result within the Ginzburg-Landau formalism that takes into account the reduction of the correlation length by the magnetic field. In this regime, the amplitude fluctuations are described as evanescent Cooper pairs arising from free electrons with quantized cyclotron orbits[4]. In our experiment, we can clearly distinguish the low-field limit – where the cyclotron length is larger than the correlation length – from the high-field limit, where the correlation length has been reduced from its value at zero field to a shorter value given by the magnetic length.

Figure 2 presents a contour plot (with a logarithmic scale of the colors) of the Nernst coefficient $\nu = N/B$ in the (l_B, ξ_d) plane. [Note that in contrast to Figure 1, ν and not N is plotted here]. These graphs are instructive. When $l_B > \xi_d$, the contour lines are parallel to the magnetic length axis, meaning that the Nernst coefficient depends only on ξ_d . On the other side of the diagonal, when $l_B < \xi_d$, the contour lines are parallel to the correlation length axis, meaning that the Nernst coefficient depends only on l_B . Furthermore, in both samples, the contour lines are almost symmetric with respect to the $l_B = \xi_d$ line. In other words, the Nernst coefficient appears to be uniquely determined by the correlation length, no matter whether ξ_d or l_B sets it.

Therefore, we are entitled to assume that there exists a function which links ν to the correlation length. In the zero-field limit, the latter is set by ξ_d , and we can empirically extract from our data a function $F(\xi)$ such as $F(\xi) = \alpha_{xy}/B = \frac{\nu}{R_{square}}(T, B \rightarrow 0)$. This function is shown in figure 3(upper panel). For large ξ , it is proportional to ξ^2 , in agreement with the USH expression. For small ξ , however, we find that this function becomes roughly proportional to ξ^4 . Now a remarkable observation follows : when this function $F(\xi)$ is plotted with the magnetic length l_B as argument, as shown in the lower panel of figure 3, we find that it almost describes the magnitude and the field dependence of the Nernst coefficient at high magnetic field. This demonstrate that in these two opposite limits, ($\xi \simeq \xi_d$ and $\xi \simeq l_B$), the Nernst coefficient is determined by this single function $F(\xi)$ that depends uniquely on the correlation length.

This function, extracted from the zero field data and observed to describe the data at high magnetic field, should also be valid at intermediate field, when $\xi_d \simeq l_B$. In this intermediate region, with the increasing magnetic field, the correlation length progressively evolves from ξ_d to l_B . A simple relation for ξ that verifies the conditions,

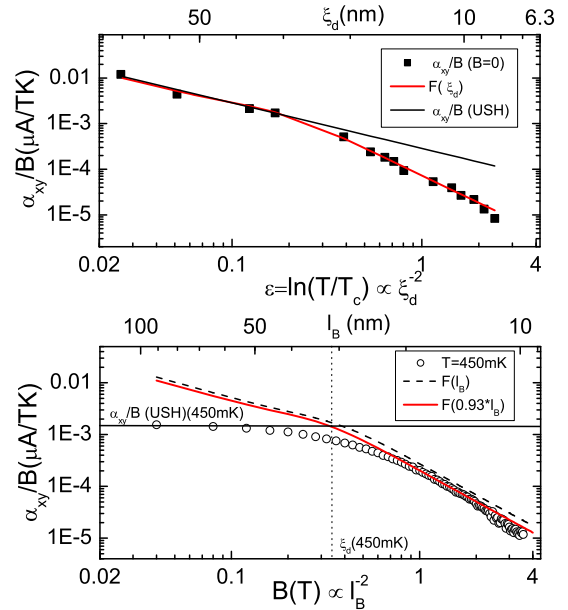


FIG. 3: Upper panel: The transverse Peltier coefficient α_{xy} divided by the magnetic field B (black squares) as a function of the reduced temperature ϵ (bottom axis) and correlation length (top axis) for sample 2 on a log-log scale. At low ϵ , the experimental data are consistent with the USH model (solid line). The function $F(\xi)$ shown as a red line is a fit to the data. Lower panel : The same function, (dot-line) plotted using l_B as its argument, $F(l_B)$, as a function of the magnetic field (bottom axis) and l_B (top axis). Note that it is consistent with the magnitude and field dependence of the data acquired at high magnetic field. The function $F(c \times l_B)$ (continuous line) describes nicely the data when $c = 0.93$. At low magnetic field, when $l_B > \xi_d$, the data deviates from $F(c \times l_B)$ to reach the field-independent value $F(\xi_d)$.

$\xi \simeq \xi_d$ when $l_B \rightarrow \infty$, and $\xi \simeq c \times l_B$ when $l_B \rightarrow 0$ is given by :

$$\frac{1}{\xi^\gamma} = \frac{1}{\xi_d^\gamma} + \frac{1}{(c \times l_B)^\gamma} \quad (2)$$

where the pre-factor c and the exponent γ are to be determined from the experimental data. The pre-factors $c = 1.12$ for sample 1 and $c = 0.93$ for sample 2 are determined such as $F(c \times l_B)$ gives precisely the field dependence of the Nernst coefficient at high magnetic field, shown figure 3. The slight difference between the pre-factors for the two samples is not understood at this stage. It appears to be larger than the experimental margin of error and suggests that other parameters not taken into account in this analysis may be involved, such as the thickness of the samples. To get the value of the exponent γ , we first note that the curves $\frac{\alpha_{xy}/B(B \rightarrow 0, T)}{\alpha_{xy}/B(B \rightarrow 0, T)}$, for temperature $T > 2 \times T_c$, collapse on a unique curve when they are plotted as a function of ξ_d/l_B , as shown figure 4. Then, using $F(\xi) \sim \xi^4$ – as previously observed for $T > 2 \times T_c$ – and using equation 2, we find that $F(\xi)/F(\xi_d) = [1 + (\frac{\xi_d}{c \times l_B})^\gamma]^{-4/\gamma}$ depends only on the ra-

tio ξ_d/l_B , and so has the appropriate functional form to describe the collapsed data. For both samples, the best fit is obtained when $\gamma = 4$, as shown Figure 4 for sample 2. Such a value of γ implies that the first non-linear correction to the field dependence of α_{xy} is proportional to B^2 (i.e l_B^{-4}), in agreement with analyticity arguments[18]. With these parameters just determined, figure 2 shows that the contour lines of equal Nernst coefficient can be described by curves of constant correlation length ξ as given by equation 2. Thus, as shown figure 4, above T_c , the magnitude of the Nernst coefficient at any temperature and magnetic field is given by this unique function $F(\xi) = \frac{\alpha_{xy}}{B}(\xi)$, determined experimentally at zero field, where the correlation length is given by equation 2.

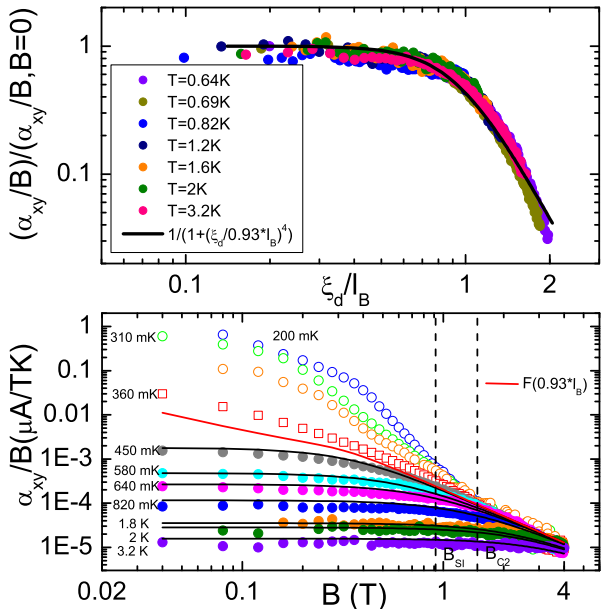


FIG. 4: Upper Panel: α_{xy}/B normalized to its zero-field value versus ξ_d/l_B for sample 2. All the data at temperatures between 430 mK and 3.2 K are shown here to collapse on $\frac{1}{1+(\xi_d/0.93*l_B)^4}$ (thick line). Lower panel: α_{xy}/B as a function of B for temperatures ranging from 200 mK to 3.2 K on a log-log scale. The function $F(\xi) = \frac{\alpha_{xy}}{B}(\xi_d)$ extracted from the data at zero field is plotted here as a function of l_B (thick red line). At high magnetic field, all the data, above and below T_c tend towards $F(c \times l_B)$. Note that $F(c \times l_B)$ is the separatrix of the data above and below T_c . Also shown is $F(\xi)$ for several values of ξ_d corresponding to different temperatures, and plotted as function of $\xi = (1/\xi_d^4 + 1/(0.93 * l_B)^4)^{-1/4}$.

Figure 4 also shows that the magnitude and field dependence of the Nernst signal, measured for temperatures $T < T_c$ and high magnetic field ($B > B_{c2}$), can also be described by $F(c \times l_B)$. In particular, we see that the Nernst data measured at a temperature close to T_c follows closely the curve $F(c \times l_B)$ on a wide magnetic field range; this is expected for the diverging Ginzburg-Landau correlation length when approaching T_c . It is remarkable to note that the curve $F(\xi)$, extracted from the data at zero-field, and plotted as a function of l_B ,

gives precisely the separatrix between the curves $\frac{\alpha_{xy}}{B}(B)$ measured above and below T_c . Below T_c , α_{xy}/B joins the function $F(c \times l_B)$ at a critical field $B_{c2} \simeq 1.5$ T, which is larger than the critical field of the superconductor-insulator transition, $B_{SI} = 0.91$ T, defined as the crossing field of $R(B)$ curves[11].

The overall consistency of this analysis demonstrates that the off-diagonal component of the Peltier tensor, α_{xy} , is set by ξ_d over a wide temperature range. As noticed previously, when ξ_d is large, α_{xy} is consistent with USH expression. However, below a correlation length of the order of ξ_{0d} , it deviates downward from the USH formula. Such a deviation is actually expected for theories based on the Ginzburg-Landau formalism, which are notoriously known to overestimate the effect of short-wave length fluctuations[4]. In fluctuations diamagnetism experiments, the data were observed to fall systematically below the Prange's limit above some scaling field, of the order of $0.5 \times H_{c2}$ in dirty materials, i.e. $\xi \simeq \xi_{0d}$.

Let us conclude by briefly commenting the case of cuprates. One crucial issue to address is the existence of the “ghost critical field” detected here. We note that such a field scale has not been identified in the analysis of the cuprate data[1]. However, one shall not forget that the normal state of the underdoped cuprates is *not* a simple dirty metal. The contribution of normal electrons to the Nernst signal is too large to be entirely negligible. This makes any comparison between theory and data less straightforward than the analysis performed here. Moreover, in $\text{Nb}_{0.15}\text{Si}_{0.85}$ there is a single temperature scale, T_{BCS} , for the destruction of superconductivity. In contrast, the situation in the cuprates may be complicated by the possible existence of two distinct temperature scales, the pairing temperature and a Kosterlitz-Thouless-like temperature leading to a phase-fluctuating superconductor[17].

To summarize, in the regime of short-lived Cooper pairs, the Nernst coefficient was found to only depend on the superconducting correlation length. We could clearly distinguish the regime where the correlation length is set by the Ginzburg-Landau correlation length at zero-field from the high-field regime where the correlation length is set by the magnetic length. In the intermediate region where $\xi_d \simeq l_B$, the correlation length is a simple combination of these two lengths. These results demonstrate that the Nernst signal observed at high field and temperature in amorphous films of $\text{Nb}_{0.15}\text{Si}_{0.85}$ is generated by superconducting fluctuations characterized by short-lived Cooper pairs, implying both amplitude and phase fluctuations of the superconducting order parameter.

We acknowledge useful discussions with S. Caprara, M.V. Feigelman, M. Grilli, D. Huse, S. Sondhi, I. Usishkin and A.A. Varlamov. This work was partially supported by Agence Nationale de la Recherche and Fondation Langlois through “Prix de la Recherche Jean Langlois”.

[1] Y. Wang, L. Li, and N. P. Ong, Phys. Rev. B **73**, 024510 (2006).

[2] R. E. Glover, Physics Letters A **25**, 542 (1967).

[3] J. P. Gollub, M. R. Beasley, R. Callarot, and M. Tinkham, Physical Review B **7**, 3039 (1973).

[4] W. J. Skocpol and M. Tinkham, Reports on Progress in Physics **38**, 1049 (1975).

[5] V. J. Emery and S. A. Kivelson, Nature **374**, 434 (1995).

[6] A. Pourret, H. Aubin, J. Lesueur, C. A. Marrache-Kikuchi, L. Bergé, L. Dumoulin, and K. Behnia, Nature Physics **2**, 683 (2006).

[7] K. Behnia, M. Measson, and Y. Kopelevich, cond-mat p. 0611136 (2006).

[8] I. Ussishkin, S. L. Sondhi, and D. A. Huse, Phys. Rev. Lett. **89**, 287001 (2002).

[9] S. Marnieros, L. Bergé, A. Juillard, and L. Dumoulin, Physical Review Letters **84**, 2469 (2000).

[10] H. L. Lee, J. P. Carini, D. V. Baxter, W. Henderson, and G. Gruner, Science **287**, 633 (2000).

[11] H. Aubin, C. A. Marrache-Kikuchi, A. Pourret, K. Behnia, L. Bergé, L. Dumoulin, and J. Lesueur, Phys. Rev. B **73**, 094521 (2006).

[12] R. P. Huebener and A. Seher, Physical Review **181**, 710 (1969).

[13] A. P. A. Kapitulnik and G. Deutscher, J. Phys. C: Solid State Phys. **18**, 1305 (1985).

[14] C. Carballoira, J. Mosqueira, A. Revcolevschi, and F. Vidal, Physical Review Letters **84**, 3157 (2000).

[15] A. Schmid, Physical Review **180**, 527 (1969).

[16] R. E. Prange, Physical Review B **1**, 2349 (1970).

[17] D. Podolsky, S. Raghu, and A. Vishwanath, cond-mat/0612096 (2006).

[18] M. Feigelman, Private Communication